Hollow-Beam Klystron Design for the International Linear Collider

Stanley Humphries
Field Precision LLC, Albuquerque, NM 87192 USA
and
Patrick Ferguson
MDS Company, Oakland, CA 94611 USA

Abstract **We describe the capabilities of an integrated software suite for the design of high-power klystrons. As an application example, the codes are applied to a 10 MW, 1.3 GHz hollow-beam klystron to meet the requirements of the International Linear Collider. The hollow-beam approach allows high beam current (140 A) in a compact package with moderate gun voltage (120 kV). The benchmark system has an interaction length of 0.92 m, 47 dB gain and 63% inherent efŒciency (excluding contributions of a biased beam collector). We discuss a electron gun design to generate a narrow annular beam with relatively small axial energy spread.**

I. Introduction

We have carried out computational studies of a hollow-beam klystron to meet the requirements of the International Linear Collider[1], a multinational project to develop a terascale electron-positron collider. The following technical goals for an RF tube are the current ones listed by the U.S. Department of Energy:

- Generate 10 MW of power at 1.3 GHz.
- Operate for a long pulse (1-3 ms) required to Œll the superconducting cavities.
- Achieve 65% energy conversion efŒciency.
- Occupy a minimum volume with manageable beam focusing magnets.

Conventional klystrons cannot meet the requirements. Our studies with the KLSC code[2], [3] show that a device to meet the power and efŒciency targets requires an electron gun operating at $\sim$190 kV. The combination of voltage, electric Œeld on the focus electrode and pulse length exceed the electron-gun breakdown criterion documented in Ref.[4].

A moderate gun voltage is required for a conservative design. At 120 kV, the required beam current is 140 A. The associated strong space-charge forces and high beam potential limit the klystron efŒciency. There are three paths to reduce the effects of beam-generated forces:

- Multiple-beams.
- Extended sheet beam.
- Hollow beam.

The multi-beam approach requires multiple cathodes and carefully designed focusing electrodes to counteract beam interactions. The device involves a complex mechanical system with considerable wasted space and a large-volume focusing magnet. Sheets beams require signiŒcant advances in beam physics, particularly the design of fully three-dimensional injectors and focusing systems that can maintain beam uniformity in the presence of non-linear transverse forces.

We believe that the hollow-beam klystron (HBK) is a simple and conservative option to meet the ILC goals. The device requires only a single cathode and transport tube of moderate diameter. The space-charge potential of a beam sets limits on the axial energy spread, and hence the klystron efŒciency. The potential of a hollow beam may be signiŒcantly lower than that of a solid beam. For example, a beam with inner radius equal to 80% of the outer radius has a space-charge potential that is only 11% of the value for a solid beam with the same outer radius and current[5]. Hollow beams also have an advantage with regard to their interaction with the cavity Œelds. Electron bunching is almost totally axial, leading to reduced beam voltage and a shorter circuit. With regard to technical risk, there is a long history of the successful use of hollow beams in klystrons and traveling wave tubes, both conventional and pulsed-power devices [6]-[12].

II. Code capabilities

Figure 1 shows the organization of the high-power klystron design suite. We have combined existing codes and created streamlined interfaces for direct data transfer. The Œrst step in a solution is to apply WAVESIM to a preliminary design of the input, gain and output cavities. The code performs two-dimensional, Œnite-element frequency-domain solutions. Field distributions are passed to the particle-in-cell code KLSC. This code is used to optimize RF performance, seeking the peak efŒciency consistent with conservative Œeld levels. The effort sets goals for the injected beam properties. A self-consistent injector design is performed with the TRAK code. The resulting input beam distribution is used for reŒned KLCS calculations. Finally, the exit electron distribution is transferred to to TRAK for the collector design. We shall discuss each code component in turn.

WAVESIM Œnds electromagnetic Œelds in cylindrical or planar structures at speciŒed frequencies. A conformal mesh and Œnite-element techniques are applied for high accuracy. WAVESIM handles both bounded and free-space calculations. The dielectric constant and magnetic permeability of materials are represented as complex numbers, so the code can determine resonant frequencies and Q values with volumetric losses. (Fig. 2). WAVESIM generates Œles of Œeld values on a rectangular for direct transfer to KLSC.

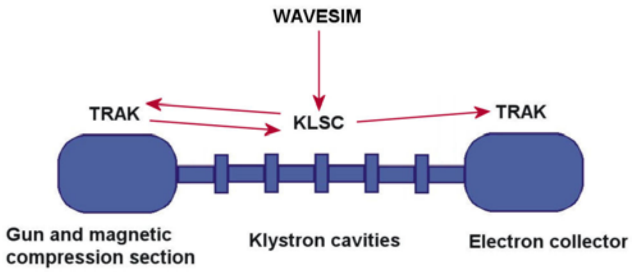

Fig. 1. Program components and data œow in the high-power klystron design suite.

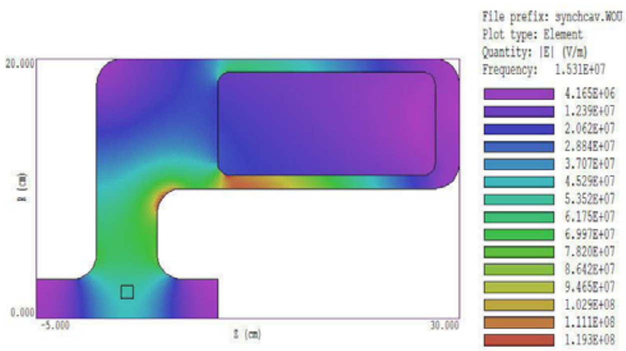

Fig. 2. WAVESIM ˘ element plot of $|\mathbf{E}|$ for the TM_{010} mode in a cavity with a lossy ferrite.

The $2^1/_2$ dimensional fully relativistic program KLSC (*klystron large-signal code*) is used for the design of the interaction circuit of the beam and RF Œelds. The program, written by Bruce Carlsten for MDS Company, addresses solid or hollow electron beams with either solenoid or periodic permanent magnetic focusing. KLSC has been extensively benchmarked. For example, in a comparison with experimental results for a 150 MW S-band klystron at the Stanford Linear Accelerator Center, the measured efŒciency was 41.7% and the measured saturated gain was 54 dB. KLSC predicted an efŒciency of 42.9% and a saturated gain of 55.9 dB.

KLSC uses a uniform rectangular mesh to calculate space-charge Œelds and advances Œelds according to the full Maxwell equations. Particles in a single RF period travel along the mesh following the Lorenz force equation. A charge-conserving algorithm is used to Œnd the space-charge Œelds and the drive current is determined from the particle motion on the mesh. The cavity RF Œelds calculated by WAVESIM are superimposed on the mesh, so that both space-charge and RF Œeld forces play a role in advancing particle motion. Particle motion is used to Œnd the driven modulation of the RF cavities. An iteration scheme is applied to Œnd the Œeld amplitude that leads to self-consistent particle motion.

Detailed modeling of the electron injector and magnetic compression section to match the beam to the klystron is critical for the success of the hollow-beam approach. The TRAK has several useful features for the application: 1) Œnite-element Œeld calculations on conformal meshes for

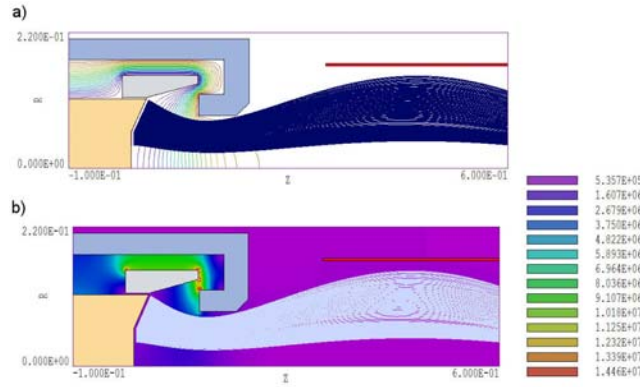

Fig. 3. TRAK simulation of the gun and matching section of an annular-beam traveling-wave tube: 1.37 A at 5.8 kV. *a*) Electrodes, equipotential lines and model electron orbits. *b*) Background shows elements color-coded by $|\mathbf{E}|$.

high accuracy, 2) advanced Child-law emission methods for a good representation of electron trajectories near the cathode edge[13] and 3) ability to use numerically-exact magnetic Œeld distribution for full nonlinear effects. TRAK also includes Monte Carlo routines for secondary electrons to model collectors.

The simulation of Fig. 3 illustrates some TRAK capabilities. The illustration shows the gun and magnetic matching section for a commercial, hollow-beam traveling-wave tube developed by C. Everleigh at Pendulum Electromagnetics. The tube shares common features with our proposed approach to the ILC klystron: an annular cathode with focusing electrodes and capture in a rising magnetic Œeld. The device produces 2.5 kW with an efŒciency of 32%. At a voltage of 5.8 kV, the beam current is 1.35 A. The magnetic Œelds rises from 600 G at the cathode to a uniform value of 900 G within the helix. The TRAK prediction of space-charge-limited total current is 1.37 A, within 1.5% of the measured value.

III. RF Interaction Circuit Design

We have used KLSC to simulate hollow beams in 5-cavity and 7-cavity circuits for the anticipated parameters of the ILC klystron. Table 1 lists results for the 7-cavity circuit. Note that the beam voltage and beam current at a beam perveance of 3.37 μperv are identical to the beam voltage and composite beam current for proposed multiple-beam klystrons. Note also that the beam area convergence is a modest 6:1, considerably lower than the Œgure of $50:1$ for the multiple beam devices. Furthermore, the circuit length from the input cavity gap to the output cavity gap is only 0.92 m, comparable to the circuit lengths for the multiple-beam klystrons currently in development. For this preliminary design, we have obtained an electronic efŒciency of 63% giving an RF output power of 10.6 MW with a modest saturated gain of 47 dB. The simulations used eight current rings that traversed the length of the circuit with seven double-reentrant cavities. Figure 4 shows the evolution of particle trajectories. With a uniform axial magnetic Œeld of 2000 Gauss, the beam was well focused with little growth in

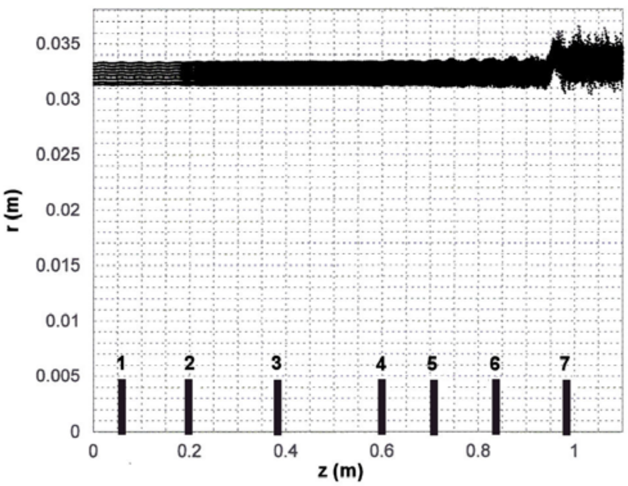

Fig. 4. Trajectories for eight electron rings traversing the 7-cavity circuit. The outer boundary is at the drift-tube radius, cavity midplanes are indicated.

TABLE I

BENCHMARK KLSC CALCULATION FOR THE ILC KLYSTRON

Quantity	Value
Beam voltage, V_b	120 kV
Beam current, I_b	140 A
Drift tube radius	3.81 cm
Beam outer radius, r_o	3.35 cm
Beam inner radius, r_i	3.12 cm
Beam current density	30 A/cm^2
Cathode current density	≤ 5 A/cm^2
Beam area convergence	$\geq 6:1$
Maximum RF efŒciency	63.1%
Maximum RF output power	10.59 MW
Saturated gain	47 dB
RF circuit length (Gap 1 - Gap 7)	0.92 m
Magnetic focusing Œeld	2000 G

radial envelope oscillations (a problem often observed with solid beams). As a consequence, the bunching was almost totally axial.

IV. ELECTRON GUN DESIGN

High-power microwave experiments with hollow electron beams often utilize magnetron-type guns. This approach is unfavorable for the ILC accelerator application because the resulting beams have high transverse energy and require strong guiding magnetic Œelds. Furthermore, the spread in axial kinetic energy reduces the efŒciency of the device. As an alternative, we are following an approach based on experiments by A.V. Agafonov[14]. Here, an axially-directed annular electron beam was created with a Pierce-type electrode system and magnetically-compressed for transport in the device. Agafonov describes experiments where annular beams with 100 A current, 400 keV kinetic energy and aspect ratio $r_i/r_o = 0.72$ were compressed by an area factor exceeding 100:1 and successfully transported in a Œeld of about 1 tesla. In comparison, our application is easier because there is smaller area compression, but more difŒcult because 1) the beam perveance is higher and 2) the transport magnetic Œeld is lower. Furthermore, we must ensure low transverse

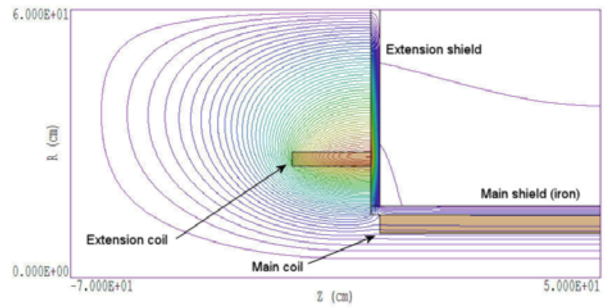

Fig. 5. Solenoid transition to the injector. Shield extension and large-radius coil give a gradual expansion of the Œeld lines.

energy. As a result, a more sophisticated gun design is necessary.

We review a benchmark calculation that illustrates the nature of the electron gun and its design feasibility. In contrast to the Agafonov conŒguration, the gun has an inclined annular cathode for injection along the local Œeld-line direction. The Œrst task is to Œnd a solenoid conŒguration with gradual Œeld-line expansion in the injector region. Figure 5 shows one option. The main solenoid has a relatively small diameter. The coil has inner radius 10.0 cm and outer radius 14.0 cm with current of 160 kA-turn/m to generate a central Œeld of 0.2 tesla. The Œeld lines at the ends of a bare solenoid expand too rapidly for smooth compression of the injected beam. The system of Fig. 5 has an extension of the iron shield and a larger diameter trim coil. With the current of the extension coil set to 64 kA-turn, Œeld uniformity is preserved to the end of the solenoid and upstream Œeld lines expand gradually.

Given the shape of the transition Œeld, we identify magnetic Œeld lines inside the solenoid with radii equal to the inner and outer dimensions of the target annular beam. In the solenoid, the lines have average radius r_0 and radial separation Δr_0. We trace the line backward into the injection region, recording values of the average radius r, the radial separation Δr and the inclination angle θ. Here, θ is the angle between a unit vector pointing in r and a vector that is normal (on average) to the Œeld lines. The ratio of the area of the inclined cathode compared to the area of the beam in the solenoid is given by

$$R_A = \left(\frac{r}{r_0}\right) \left(\frac{\Delta r}{\Delta r_0}\right) \left(\frac{1}{\cos\theta}\right). \quad (1)$$

The cathode should be located at the axial position where R_A equals the target compression ratio of 6. For the Œeld geometry of Fig. 5, the position is 46 cm upstream from the solenoid entrance with a cathode inclination angle of 18°. The upper portion of Figure 6 shows an electrode geometry determined after several iterations. Focusing electrodes at the Pierce angle (22.5°) bracket the inclined cathode. The cathode assembly is at potential $\phi = -120$ kV. An inner anode electrode is necessary to prevent strong radial beam expansion in unbalanced aperture Œelds.

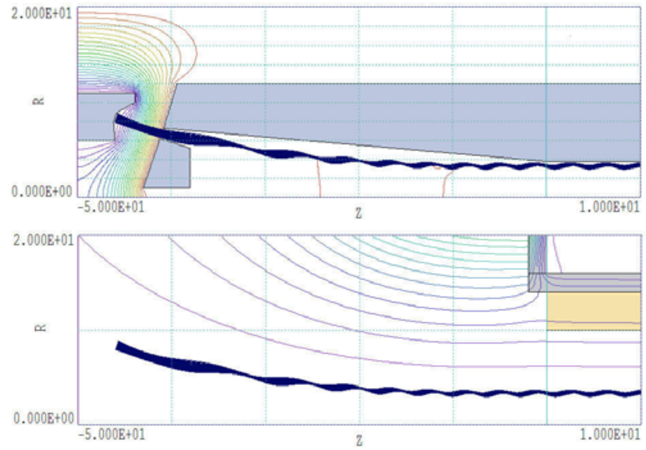

Fig. 6. Initial design for an immersed, annular beam gun with Pierce-type focusing electrodes and an inclined cathode. Top: Electrodes, model electron orbits and equipotential lines of the electric-Œeld solution. Bottom: Magnetic Œeld solution: coils, iron, model electron orbits and Œeld lines.

The **TRAK** calculation of the model electron orbits in Fig. 6 is fully self-consistent, including effects of space charge and beam generated magnetic Œelds. The space-charge-limited current is 138.7 A. The solution is encouraging but not perfect. The beam within the solenoid has a thickness of about 3.0 mm compared to the target value of 2.3 mm. The beam exhibits envelope oscillations ˘ the amplitude is ± 1.4 mm on the outer boundary. These oscillations are an unavoidable consequence when high-current beams are created with immersed injectors[5]. Such a beam must expand radially to provide an axial velocity components for a radial magnetic force that balances the space charge force. We have two goals for improvement of the gun design: 1) modify the shape and radius of extension shield and coil to minimize their size and the required drive current and 2) Œne-tune the shape of injector electrodes to reduce radial oscillations of the transported beam.

REFERENCES

[1] DOE/NSF High-energy Physics Advisory Panel, **Discovering the Quantum Universe, The Role of Particle Colliders**, report available at http://www.interactions.org/quantumuniverse/qu2006/

[2] B. Carlsten, P. Ferguson and D. Sprehn, *Accuracy of the equivalent-circuit model using a Œxed-beam impedance for klystron gain cavities*, IEEE Trans. Plasma Sci. **26**, 1745 (1998).

[3] B. Carlsten and P. Ferguson, *Large-signal simulations using KLSC*, **Proc. Particle Accel. Conf.**, 3129 (1997).

[4] R. Latham, **High-voltage Vacuum Insulation** (Academic Press, London, 1995), 428.

[5] S. Humphries, **Charged Particle Beams** (Wiley, New York, 1990), Sect. 5.3.

[6] W. Beaver, G. Caryotakis, G. Huffman and N. Taylor, *An experimental wide-band klystron employing a high perveance hollow beam*, **Proc. Electron Devices Meeting**, 72 (1959).

[7] L. Fox, *Development of a broadband hollow beam, modulating anode L-band klystron at the multi-megawatt level*, **Proc. Electron Devices Meeting**, 20 (1963).

[8] E. Demmel, *Some studies of a high-perveance hollow-beam klystron*, IEE Trans. Electron Devices **11**, 66 (1964).

[9] A. Dovbnya, *et.al.*, *On the creation of cathode units for the X-band klystron*, **Proc. Particle Accelerator Conf.**, 1107 (2003).

[10] M. Friedman, J. Krall, Y. Y. Lau, and V. Serlin, *EfŒcient generation of multigigawatt RF power by a klystronlike ampliŒer*, Rev. Sci. Instrum. **62**, 171 (1990).

[11] J. Nation, *On the coupling of an high-current relativistic electron beam to a slow wave structure*, Appl. Phys. Lett. **17**, 491 (1970).

[12] K. Hendricks, *et.al.*,*Generation, propagation and diagnostics of a long pulse annular electron beam for an HPM source*, **Proc. Pulsed Power Conf.**, 1147 (2003.).

[13] S. Humphries, *Numerical modeling of space-charge-limited charged-particle emission on a conformal triangular mesh*, J. Comp. Phys. **125**, 448 (1996).

[14] A.V. Agafonov, E.G. Krastelev, A.N. Lebedev, V.S.Voronin, P.N. Lebedev, *Forming of precision thin-wall hollow electron beams for microwave generators*, **XVI Int l. Workshop Charged-particle Linear Accelerators**, 507 (1999).